Review Article

On the Study of Nyquist Contour Handling Sampled-Data Control System Real Poles and Zeros

Yossawee Weerakamhaeng*
Department of Electrical and Computer Engineering, Faculty of Engineering,
Thammasat University Rangsit Campus, Khlong Nueng, Khlong Luang, Pathum Thani 12120, Thailand

Abstract

The Nyquist plot is a crucial tool in the analysis and design of linear time-invariant (LTI) and linear shift-invariant (LSI) control systems such as in the relative stability analysis, gain margin, phase margin and robust stability analysis. In the Nyquist plot plane, certain positions must be determined, such as the real axis crossings. These positions are sometimes hidden or ambiguous because of the large span in the magnitude of the Nyquist plot over the entire frequency range. As a result, the Nyquist sketch is introduced as a guide to manually draw the Nyquist plot regarding the qualitative graphical representations such as high frequency asymptote, low frequency asymptote (DC gain point), real and imaginary axis crossings. For LTI control systems or continuous-time control systems, the Nyquist sketch is demonstrated in several studies. However, for LSI control systems or discrete-time control systems, few references mention the Nyquist sketch and only in a vague manner. This study delineates extensively the sketch of the Nyquist plot or the Nyquist sketch for discrete-time control systems extending to the sampled-data control systems when the loop pulse transfer function possesses some real poles and/or zeros outside the unit circle in the z-plane.

Keywords: Nyquist contour; Nyquist sketch; Nyquist plot; relative stability; unit circle; stability of discrete-time systems; Nyquist stability criterion

Nomenclature

$GH(z)$	The loop pulse transfer function.	T	Sampling period in seconds.
$G_p(s)$	Transfer function of a continuous-time plant.	$R(z)$	The z-transform of the input sequence to the system.
$H(s)$	Transfer function of a sensor in the feedback path.	$C(z)$	The z-transform of the output sequence of the system.
		$P(z)=1+GH(z)$	The characteristic equation of the

***Correspondence** : wyossawe@engr.tu.ac.th DOI 10.14456/tijsat.2016.30

	discrete-time control system.
Ω	The digital angular frequency (rad/s).
$r \in R$	A real variable.
$\varepsilon \in R$	A miniature-valued real variable.
$\beta \in R$	A miniature-valued real variable.
finite	A constant value greater than zero but less than infinity.
$\mathrm{Im}[GH(q)]$	The imaginary part of $GH(q)$
$\mathrm{Re}[GH(q)]$	The real part of $GH(q)$
$\mathrm{Im}[GH(x+jy)]$	The imaginary part of $GH(x+jy)$
$\mathrm{Re}[GH(x+jy)]$	The real part of $GH(x+jy)$
$\angle(GH(q))$	The angle of the $GH(q)$ vector in the $GH(z)$-plane
$2\pi^+ = (2\pi)^+$	The quantity a little greater than 2π such that $2\pi^+ - 2\pi = 0^+$
0^-	The quantity a little less than 0 such that $0 - 0^- = 0^+$
$e^{j0^-} = e^{j(0)^-} = e^{-j(0)^+}$	The unit vector aligned with the miniature negative angle.

1. Introduction

With the publication of "Regeneration Theory" by H.Nyquist [1], who used the term "Regeneration" as synonymous with "feedback", the general stability problem was found to be solved by the well-known Nyquist stability criterion that he established as well. The Nyquist stability criterion has been used to examine the relative stability of continuous-time control systems [2], [3]. With the graphical tool called "Nyquist plot", the relative stability analysis of systems involving time delays is obviously comprehensible. Its effectiveness depends upon the correct shape of the Nyquist plot of the loop transfer function. With the introduction of microprocessors and microcontrollers, continuous-time control systems have evolved into the mixture of the continuous-time plants and the discrete-time controllers bridged by the sampling process. The new control systems are called the sampled-data control systems. Researchers facilitated the analysis and design of the sampled-data control systems by converting them into the discrete-time control systems. The analysis and design of discrete-time control systems in frequency domains is done in the z-plane. The relative stability property of the discrete-time control system still relies on the Nyquist stability criterion considering the unit circle in the z-plane as the reference boundary for constructing the Nyquist contour prior to the Nyquist plot as the mapping result. In [4], the Nyquist contour is defined as the unit circle with the imposed constraint of the equal

order of both the numerator and denominator constituting the characteristic equation as a rational function of the complex variable z. Then the number of zeros (poles of system) outside the unit circle of the characteristic equation are inferred from the ones inside the unit circle with additional information by using the Principle of Argument theorem. However, there are some situations in which the imposed constraint is invalid, yielding an incorrect result from the relative stability test. In order to overcome the problem, some researchers [5], [6], [7], [8], [9] and [10] redefined the Nyquist contour surrounding the entire area of the z-plane excluding the unit circle(enclosing the exterior of the unit circle) without the aforementioned constraint but with some segments traversing on the real axis of the z-plane outside the unit circle. These segments make the Nyquist contour exclude real poles and zeroes of $GH(z)$ outside the unit circle leading to the relative stability test error. Although there are software packages that assist in plotting, all the input data must be numerical values and it is very hard to quantitatively explain the infinite quantities. It always happens that the obtained Nyquist plot is unreadable when the system possesses poles on the real axis outside the unit circle in the z-plane due to the large span in the magnitude of the polar plot over the entire frequency range. Accordingly, this study delineates extensively the sketch of the Nyquist plot or the Nyquist sketch for discrete-time control systems extending to the sampled-data control systems considering poles and zeroes, especially when some of the real poles and/or zeros of $GH(z)$ are outside the unit circle in the z-plane.

2. Nyquist Contours and Qualitative Graphical Representations

Figure 1. shows a basic sampled-data control system consisting of a continuous-time plant $G_p(s)$ with a zero-order hold, $\frac{1-e^{-sT}}{s}$ leading it. $G(s)$ is defined as:

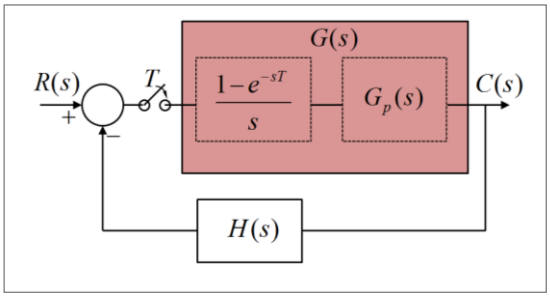

Figure 1. A basic sampled-data control system.

$$G(s)=\frac{1-e^{-sT}}{s}G_p(s) \qquad (1)$$

The error signal $R(s)-C(s)$ is sampled by a sampler with the sampling period of T s. The feedback path represents the sensor transfer function $H(s)$. Converting this system to a discrete-time control system results in the pulse transfer function relating the input $R(z)$ to output $C(z)$ as:

$$\frac{C(z)}{R(z)}=\frac{G(z)}{1+GH(z)} \qquad (2)$$

The characteristic equation $P(z)=1+GH(z)$ describes the behaviors including the relative stability of this system. For the relative stability analysis, the system becomes unstable when there is at least one pole (one zero of $P(z)$) of the system outside the unit circle in the z-plane. The Nyquist stability criterion implies the number of zeros of $P(z)$ from the number of encirclements of the Nyquist plot of the loop pulse transfer function $GH(z)$ around point $GH(z)=-1$ in the $GH(z)$ plane. The Nyquist plot can be

considered as the graphical result of the mapping by the complex function $GH(z)$ from the Nyquist contour in the z-plane to the Nyquist plot in the $GH(z)$-plane. The scope of this paper considers $GH(z)$ as a rational polynomial pulse transfer function able to be expressed in three different forms as follows:

- Polynomial form:

$$GH(z)=\frac{b_m z^m+b_{m-1}z^{m-1}+\ldots+b_1 z+b_0}{z^h(a_n z^n+a_{n-1}z^{n-1}+\ldots+a_1 z+a_0)} \quad \ldots\ldots\ldots\ldots\ldots\ldots \quad (3)$$

- Zero-pole-gain form:

$$GH(z)=k\frac{(z-z_1)(z-z_2)\ldots(z-z_m)}{z^h(z-p_1)(z-p_2)\ldots(z-p_n)} \quad \ldots\ldots\ldots\ldots\ldots\ldots \quad (4)$$

- Time-constant form:

$$GH(z)=\tau\frac{(1-\tau_{1N}z^{-1})(1-\tau_{2N}z^{-1})\ldots(1-\tau_{mN}z^{-1})}{z^h(1-\tau_{1D}z^{-1})(1-\tau_{2D}z^{-1})\ldots(1-\tau_{nD}z^{-1})} \quad \ldots\ldots\ldots\ldots\ldots\ldots \quad (5)$$

This study proposes to construct the Nyquist contour in such a way that it surrounds the entire area of the z-plane excluding the unit circle (enclosing the exterior of the unit circle), embraces all the real poles and zeros of $GH(z)$ outside the unit circle in the z-plane and complies with the frequency response plot of this system by the Bode plot where $z=e^{j\Omega}$, $|GH(z)|=|GH(e^{j\Omega})|$ $\angle GH(z)=\angle GH(e^{j\Omega})$ and $0\le\Omega\le 2\pi$ or $-\pi\le\Omega\le\pi$ rad/sample (Ω is the digital angular frequency). The marvelous segment of the contour proposed by this study is the segment parallel to the real axis of the z-plane but raised above this real axis by a tiny amount of ε.

2.1 Nyquist contour when no poles of $GH(z)$ on the unit circle or on positive real axis at $z=1$ in the z- plane

Consider the situation when no poles of $GH(z)$ are on the unit circle or on the positive real axis at $z=1$ in the z-plane. For illustration, a real pole, $z=p_i$ and a real zero, $z=z_s$ are given**.** The Nyquist contour can be drawn as in Figure 2. The contour comprises 4 segments, namely

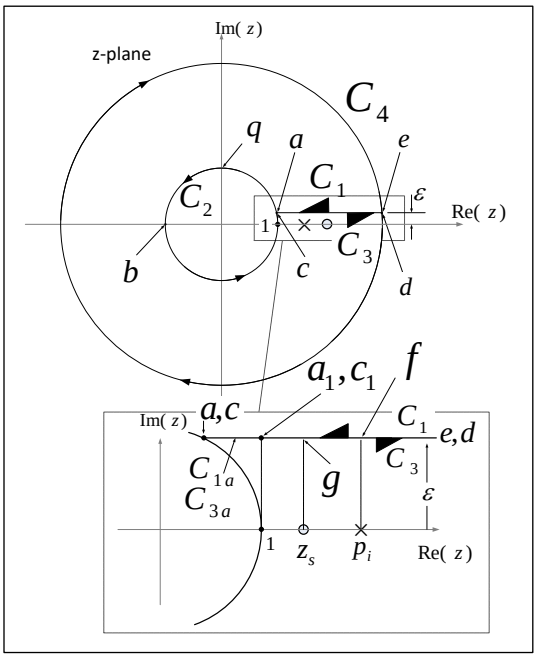

Figure 2. Nyquist contour when no pole of $GH(z)$ on the unit circle or on positive real axis from $z=1$ in the z-plane.

2.1.1 C_1 segment:

This segment is a straight line, a short distance (ε) above the real axis of the z-plane , traversing from $z\to\infty+j\varepsilon$ (point d, e) to $z=1+j\varepsilon$ (point a1, c1). It is characterized by

$$z=\frac{1}{r+1}+j\varepsilon \quad \ldots\ldots\ldots\ldots\ldots\ldots(6)$$

Where $-1\le r\le 0$ and $\varepsilon\to 0(\varepsilon=0^+)$. When $r=-1$, $z\to\infty+j\varepsilon$ and it is represented by point e

in Figure 2. By the zero-pole-gain form of $GH(z)$,

$$\angle k = \begin{cases} 0 \quad rad\,; k \geq 0 \\ \pm\pi \quad rad\,; k < 0 \end{cases} \qquad \text{.....} \quad (7)$$

For most physical systems, $k > 0$ and therefore

When $m < (h+n)$ **and** $k > 0$**,**

$$GH(z) = GH(e) \approx \frac{z^m}{z^h z^n} e^{j\angle k} \approx 0^+ - j\beta \quad ; \beta \to 0\,(\beta = 0^+) \qquad \text{.....} \quad (8)$$

When $m > (h+n)$ **and** $k > 0$**,**

$$GH(z) = GH(e) \approx \frac{z^m}{z^h z^n} e^{j\angle k} \to \infty + j\beta \quad ; \beta \to 0\,(\beta = 0^+) \qquad \text{.....} \quad (9)$$

When $m = (h+n)$ **and** $k > 0$**,**

$$GH(z) = GH(e) \approx \frac{z^m}{z^h z^n} e^{j\angle k} \to 1 \qquad \text{.....} \quad (10)$$

When $r = 0$, $z = 1 + j\varepsilon$ or $z \approx 1$ it is represented by point a_1. By the polynomial form of $GH(z)$,

$$GH(z) = GH(a_1) \approx \frac{b_m + b_{m-1} + \ldots + b_1 + b_0}{a_n + a_{n-1} + \ldots + a_1 + a_0} \qquad \text{.....} \quad (11)$$

2.1.1.1 $\angle(GH(z))$ **on the intervals over the real poles and zeros of** $GH(z)$

On the C_1 segment, $\angle(GH(z))$ does not depend on the complex conjugate pole pairs or zero pairs because of the angle cancellation for each pair. Now, considering when $z = z_i^+ + j\varepsilon$,

$$|z - z_i| = |z_i^+ + j\varepsilon - z_i| = |0^+ + j\varepsilon| \approx 0 \qquad \text{.....} \quad (12)$$

$$\angle(z - z_i) = \angle(0^+ + j\varepsilon) \approx 0^+ rad \qquad \text{.....} \quad (13)$$

When $z = z_i + j\varepsilon$,

$$|z - z_i| = |z_i + j\varepsilon - z_i| = |0 + j\varepsilon| \approx 0 \qquad \text{.....} \quad (14)$$

$$\angle(z - z_i) = \angle(0 + j\varepsilon) \approx \frac{\pi}{2} rad \qquad \text{.....} \quad (15)$$

When $z = z_i^- + j\varepsilon$,

$$|z - z_i| = |z_i^- + j\varepsilon - z_i| = |0^- + j\varepsilon| \approx 0 \qquad \text{.....} \quad (16)$$

$$\angle(z - z_i) = \angle(0^- + j\varepsilon) \approx \pi^- rad \qquad \text{.....} \quad (17)$$

Graphical representation of $\angle(0^+ + j\varepsilon) = 0^+ \quad rad$ can be depicted as in Figure (3). From Eq. (12), Eq. (13), Eq. (14), Eq. (15), Eq. (16), and Eq. (17), it means that when travelling on C_1 segment**,** $\angle GH(z)$ is changed by an amount of $\frac{\pi}{2} rad$ at the position directly over each zero or pole of $GH(z)$ on the real axis of the

z-plane. $|GH(z)| = 0$ at the position exactly over each zero, whereas $|GH(z)| \to \infty$ at the position exactly over each pole. Just after passing the position directly over each zero or pole, $\angle GH(z)$ is changed by an amount of $\pi\ rad$ with the same $|GH(z)|$ as at the position directly over each zero or pole. Consecutively, in the Nyquist sketch, $|GH(z)|$ is changed abruptly at the position of z over either the pole or the zero and preserved at that magnitude until $\angle GH(z)$ is changed by a greater amount of $\frac{\pi}{2}\ rad$ from that position.

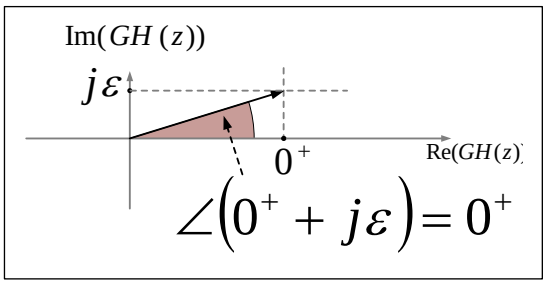

Figure 3. Graphical representation of $\angle(0^+ + j\varepsilon) = 0^+ \quad rad$.

2.1.1.2 $|GH(z)|$ on the intervals over the real poles and zeros of $GH(z)$

Moving on the C_1 segment results in the variation of $|GH(z)|$ as follows:

- Moving from point e to a position directly over a zero: $|GH(z)|$ is varied as $0 \to finite \to 0$
- Moving from point e to a position directly over a pole: $|GH(z)|$ is varied as $0 \to finite \to \infty$
- Moving from a position directly over a zero to a position directly over a pole: $|GH(z)|$ is varied as $0 \to finite \to \infty$
- Moving from a position directly over a zero to a position directly over a zero: $|GH(z)|$ is varied as $0 \to finite \to 0$
- Moving from a position directly over a pole to a position directly over a zero: $|GH(z)|$ is varied as $\infty \to finite \to 0$
- Moving from a position directly over a pole to a position directly over a pole: $|GH(z)|$ is varied as $\infty \to finite \to \infty$

2.1.2 C_{1a} segment:

This segment is a straight line, a short distance (ε) above the real axis of the z-plane , traversing from $z = 1 + j\varepsilon$ (point a_1) to $z = 1^- + j\varepsilon, (z = e^{j0^+})$ (or point a on the unit circle) in Figure 2. It is characterized by

$$z = 1 - r + j\varepsilon \qquad \text{.....(18)}$$

Where $0 \le r \le 0^+$. When $r = 0$, $z = 1 + j\varepsilon$ (point a_1) and no pole or zero of $GH(z)$ is at $z = 1$, $GH(a_1)$ is as of Eq.(11). When $r = 0^+$, $z = 1^- + j\varepsilon$ (point a) and no pole or zero of $GH(z)$ is at $z = 1$, $GH(a)$ is as of Eq.(11).

2.1.3 C_2 segment:

This segment is characterized by

$$z = e^{j\Omega} \text{ where } 0 < \Omega \le (2\pi)^+ \qquad (19)$$

When $\Omega \to 0(\Omega = 0^+)$, $z \to 1(z = e^{j0^+})$ it is represented by point a in Figure 2.

$$GH(z) = GH(a)$$
$$= k\frac{(e^{j0^+} - z_1)(e^{j0^+} - z_2)\ldots(e^{j0^+} - z_m)}{e^{j(h0^+)}(e^{j0^+} - p_1)(e^{j0^+} - p_2)\ldots(e^{j0^+} - p_n)}$$
$$\approx \frac{b_m + b_{m-1} + \ldots + b_1 + b_0}{a_n + a_{n-1} + \ldots + a_1 + a_0}$$

..... (20)

When $\Omega = \frac{\pi}{2}$, $z = e^{j\frac{\pi}{2}} = j$ it is represented by point q. By the polynomial form of $GH(z)$,

$$GH(z) = GH(q)$$
$$= \frac{b_m j^m + b_{m-1} j^{m-1} + \ldots + b_1 j + b_0}{j^h(a_n j^n + a_{n-1} j^{n-1} + \ldots + a_1 j + a_0)}$$
$$= \mathrm{Re}[GH(q)] + j\,\mathrm{Im}[GH(q)]$$

..... (21)

$$\angle(GH(q)) = \tan^{-1}\left(\frac{\mathrm{Im}[GH(q)]}{\mathrm{Re}[GH(q)]}\right)$$

..... (22)

$$|GH(q)| = \sqrt{(\mathrm{Re}[GH(q)])^2 + (\mathrm{Im}[GH(q)])^2}$$

..... (23)

When $\Omega = \pi$, $z = -1(z = e^{j\pi})$ it is represented by point b. By the polynomial form of $GH(z)$,

$$GH(z) = GH(b)$$
$$= \frac{(-1)^m b_m + (-1)^{m-1} b_{m-1} + \ldots - b_1 + b_0}{(-1)^n a_n + (-1)^{n-1} a_{n-1} + \ldots - a_1 + a_0}$$

..... (24)

When $\Omega \to (2\pi)^+$, $z \to 1(z = e^{j2\pi+})$ it is represented by point c.

$$GH(z) = GH(c)$$
$$= k\frac{(e^{j(2\pi^+)} - z_1)(e^{j(2\pi^+)} - z_2)}{e^{j(h(2\pi)^+)}(e^{j(2\pi^+)} - p_1)(e^{j(2\pi^+)} - p_2)}$$
$$\bullet \quad \frac{\ldots(e^{j(2\pi^+)} - z_m)}{\ldots(e^{j(2\pi^+)} - p_n)}$$
$$\approx \frac{b_m + b_{m-1} + \ldots + b_1 + b_0}{a_n + a_{n-1} + \ldots + a_1 + a_0}$$

..... (25)

From Eq. (20), Eq. (21), Eq. (22), Eq. (23), Eq. (24) and Eq. (25), it is obvious that the C_2 segment in the z-plane is mapped to a curve in the $GH(z)$ plane starting from point $GH(a)$ on the real axis of the $GH(z)$ plane and moves in the direction(CCW or CW depending upon the number of zeros and poles of $GH(z)$ surrounded by this segment in the z-plane) such that the next quadrant in the $GH(z)$ plane is identified by $\angle GH(q)$. This curve continues to move to point $GH(b)$ on the real axis of the $GH(z)$ plane and ends at point $GH(c)$ which is very close to point $GH(a)$. In the $GH(z)$ plane, it is possible to locate the real axis crossings and imaginary axis crossings from this curve by letting

$$z = x + jy \qquad (26)$$

Owing to the C_2 segment being the unit circle arc, any point z on C_2 must comply with the following relation:

$$x^2 + y^2 = 1 \qquad (27)$$

By the zero-pole-gain form of $GH(z)$,

$$GH(z) =$$
$$k\frac{(x + jy - z_1)(x + jy - z_2)\ldots(x + jy - z_m)}{(x + jy)^h(x + jy - p_1)(x + jy - p_2)\ldots(x + jy - p_n)}$$
$$= \mathrm{Re}[GH(x + jy)] + j\,\mathrm{Im}[GH(x + jy)] \qquad (28)$$

The real axis crossings are obtained from the coordinates (x, y) satisfying the two following equations:

$$\mathrm{Im}[GH(x+jy)]=0 \quad (29)$$
$$x^2+y^2=1 \quad (30)$$

With the calculated (x, y) from Eq. (29) and Eq. (30), the real axis crossings in the $GH(z)$ plane are expressed as the coordinate $(GH(x+jy), 0)$.

The imaginary axis crossings are obtained from the coordinates (x, y) satisfying the two following equations:

$$\mathrm{Re}[GH(x+jy)]=0 \quad (31)$$
$$x^2+y^2=1 \quad (32)$$

With the calculated (x, y) from Eq. (31) and Eq. (32), the imaginary axis crossings in the $GH(z)$ plane are expressed as the coordinate $(0, GH(x+jy))$.

2.1.4 C_{3a} segment:

This segment is a straight line, a short distance (ε) above the real axis of the z-plane, traversing from $z=1^- + j\varepsilon, (z=e^{j0^+})$ (or point c) to $z=1+j\varepsilon$ (point c_1) in Figure 2. It is characterized by

$$z=1+r+j\varepsilon \quad (33)$$

Where $0^- \le r \le 0$. When $r=0^-$, $z=1^- + j\varepsilon$ (point c) and no pole or zero of $GH(z)$ is at $z=1$, $GH(c)$ is as of Eq.(25). When $r=0$, $z=1+j\varepsilon$ (point c_1) and no pole or zero of $GH(z)$ is at $z=1$, $GH(c_1)$ is as of Eq.(25).

2.1.5 C_3 segment:

This segment is characterized by

$$z=1+r+j\varepsilon \text{ where } 0\le r<\infty \text{ and } \varepsilon\to 0(\varepsilon=0^+) \quad (34)$$

When $r=0$, $z\to 1(z=1+j\varepsilon)$ and it is represented by point c in Fig. 2. $GH(c)$ is as of Eq.(25). When $r\to\infty$, $z\to\infty+j\varepsilon$ it is represented by point d. $GH(d)$ is the same as $GH(e)$ of Eq. (8), Eq. (9), and Eq. (10), respectively. This means that C_{3a} segment is mapped by $GH(z)$ as a point as the one mapped by C_{1a} segment and C_3 segment is mapped by $GH(z)$ into the $GH(z)$-plane with reversed direction from the one mapped by C_1 segment.

2.1.6 C_4 segment:

This segment is characterized by

$$z=re^{-j\Omega} \quad (35)$$

Where $r\to\infty$ and $0^- \le \Omega \le (2\pi)^-$. When $\Omega=0^-$, $z=re^{-j0^-}$ it is represented by point d in Fig. 2. By the zero-pole-gain form of $GH(z)$,

When $m<(h+n)$ and $k>0$,

$$GH(z)=GH(d)$$
$$\approx \frac{r^m}{r^h r^n} e^{j(\angle(k-(m0)^-+(h0)^-+(n0)^-))}$$
$$\to 0e^{j(\angle(k-(m0)^-+(h0)^-+(n0)^-))}$$
$$\to 0e^{j0^-}$$

..... (36)

When $m > (h+n)$ **and** $k > 0$,

$$GH(z) = GH(d)$$
$$\approx \frac{r^m}{r^h r^n} e^{j(\angle(k-(m0)^-+(h0)^-+(n0)^-))}$$
$$\to \infty e^{j(\angle(k-(m0)^-+(h0)^-+(n0)^-))}$$
$$\to \infty e^{-j(0^-)} = \infty e^{j(0^+)}$$
..... (37)

When $m = (h+n)$ **and** $k > 0$,

$$GH(z) = GH(d)$$
$$\approx \frac{r^m}{r^h r^n} e^{j(\angle(k-(m0)^-+(h0)^-+(n0)^-))}$$
$$\to e^{j(\angle k)} = e^{j0}$$
..... (38)

When $\Omega = (2\pi)^-$, $z = re^{-j(2\pi^-)}$ it is represented by point e. By the zero-pole-gain form of $GH(z)$,

When $m < (h+n)$ **and** $k > 0$,

$$GH(z) = GH(e)$$
$$\approx \frac{r^m}{r^h r^n} e^{j(\angle(k-(2m\pi)^-+(2h\pi)^-+(2n\pi)^-))}$$
$$\to 0e^{j(\angle(k-(2m\pi)^-+(2h\pi)^-+(2n\pi)^-))}$$
$$\to 0 - j\beta \quad ; \beta \to 0\ (\beta = 0^+)$$
..... (39)

When $m > (h+n)$ **and** $k > 0$,

$$GH(z) = GH(e)$$
$$\approx \frac{r^m}{r^h r^n} e^{j(\angle(k-(2m\pi)^-+(2h\pi)^-+(2n\pi)^-))}$$
$$\to \infty e^{j(\angle(k-(2m\pi)^-+(2h\pi)^-+(2n\pi)^-))}$$
$$\to \infty + j\beta \quad ; \beta \to 0\ (\beta = 0^+)$$
..... (40)

When $m = (h+n)$ **and** $k > 0$,

$$GH(z) = GH(e)$$
$$\approx \frac{r^m}{r^h r^n} e^{j(\angle(k-(2m\pi)^-+(2h\pi)^-+(2n\pi)^-))}$$
$$\to e^{j(\angle k)} = e^{j0}$$
..... (41)

It can be noticed that when $m \neq (h+n)$ and $k > 0$,

$$\angle GH(e) - \angle GH(d)$$
$$= -(2m\pi) + (2h\pi) + (2n\pi)$$
..... (42)

In contrast, when $m = (h+n)$ and $k > 0$,

$$\angle GH(e) - \angle GH(d)$$
$$= 0$$
..... (43)

It can be noticed that $\angle GH(e)$ of C_4 segment is different from the one of C_1 segment because the meaning of point e on the C_4 segment is the position of the locus encircling the origin of the z-plane, whereas the meaning of point e on the C_1 segment is the position of a point on the straight line in the z-plane. Considering a practical physical system(causal system), $m < (h+n)$ and $k > 0$, this means that C_4 segment in the z-plane is mapped to the miniature circular arc centering at the origin of the $GH(z)$ plane starting encircling around the origin of the $GH(z)$ plane from point $GH(d)$ with the angle of $0\ rad$ ($\angle k = 0\ rad$) and continuing to rotate CCW for an additional angle of $(-2m\pi + 2h\pi + 2n\pi)\ rad$ till the arc stops at point $GH(e)$ with the angle of $\left(k - (2m\pi)^- + (2h\pi)^- + (2n\pi)^-\right)_{rad}$.

Moreover, let the system have a pole, p_i and a zero, z_s located as in Figure 2. The Nyquist plot in this section can be illustrated as in Figure 4.

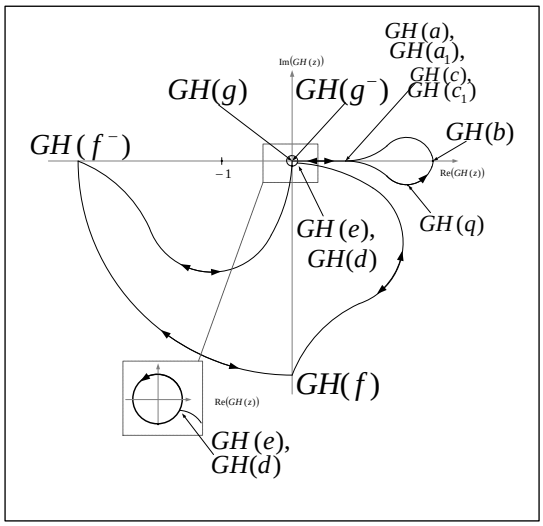

Figure 4. Nyquist plot of $GH(z)$ when no pole of $GH(z)$ on the unit circle or on positive real axis at $z=1$ in the z-plane, such a pole p_i and zero z_s located as in Figure 2. for $k>0$ and $m<(h+n)$.

By defining C_1, C_{1a}, C_3 and C_{3a} segments in these manners, only the C_2 segment plays a major role in the encirclement of $GH(z)$ around point $GH(z)=-1$ in the $GH(z)$ plane. $GH(b)$ and $GH(a)$ or $GH(c)$ are used to predict the encirclement of $GH(z)$ around point $GH(z)=-1$ in the $GH(z)$ plane with the direction of rotation indicated by $GH(q)$.

2.2 Nyquist Stability Criterion

After the Nyquist sketch from Section 2.1 is completed, the number of CCW encirclements around point $GH(z)=-1$ in the $GH(z)$ plane is countable as N (i.e., $-N$ for CW encirclements). The loop gain $GH(z)$ has the known P open loop poles with the unknown Z zeros of $P(z)$ inside the Nyquist contour or outside the unit circle in the z-plane. The rotation direction of the contour in Figure 2, when situated inside the contour, is in CW direction. By the Principle of Argument theorem,

$$N=P-Z \tag{44}$$

And therefore,

$$Z=P-N \tag{45}$$

Eq. (45) is used to determine the number of zeros of $P(z)$ inside the contour or outside the unit circle in the z-plane. **The LSI control system (discrete-time control system) is unstable if**

$$Z>0 \tag{46}$$

or

$$N\neq P \tag{47}$$

Eq. (47) is used to determine the relative stability property of the discrete-time control system.

3. Numerical Example

3.1 Example 1.

Considering a sample-data control system in Figure 1. with unity feedback $H(s)=1$, let

$$G(z)=\frac{1.0}{z-1.5}$$

Pole of $G(z)$ is at : $z=1.5$

$$\frac{C(z)}{R(z)}=\frac{G(z)}{1+G(z)}=\frac{1}{z-0.5}$$

The characteristic equation, $P(z)$ can be expressed as

$$P(z) = 1 + G(z) = \frac{z - 0.5}{z - 1.5}$$

Zero of $P(z)$ is at : $z = 0.5$

The Nyquist contour can be demonstrated as in Figure 2. The contour consists of 6 segments, namely

C_1 **segment:** referring to Eq. (6),

$z = \frac{1}{r+1} + j\varepsilon$ where $-1 \le r \le 0$ and $\varepsilon \to 0 (\varepsilon = 0^+)$. According to Eq. (8)

$$G(e) \approx 0^+ - j\beta$$

Traversing on this segment to the point directly over the pole at $z = 1.5$. This point is expressed as $z = 1.5 + j\varepsilon$

$$G(1.5 + j\varepsilon) \to \infty \angle \left(-\frac{\pi}{2} \right)$$

Continuing to point $z = 1.5^- + j\varepsilon$

$$G(1.5^- + j\varepsilon) \to \infty \angle (-\pi)$$

Continuing to point $z = 1.0 + j\varepsilon$

$$G(1.0 + j\varepsilon) \approx \frac{1}{1 - 1.5} = -2.0$$

C_{1a} **segment:** referring to Eq. (18),

$z = 1 - r + j\varepsilon$ where $0 \le r \le 0^+$ and $\varepsilon \to 0 (\varepsilon = 0^+)$. At point $z = 1.0 + j\varepsilon$

$$G(1.0 + j\varepsilon) \approx \frac{1}{1 - 1.5} = -2.0$$

At point $z = 1.0^- + j\varepsilon$

$$G(1.0^- + j\varepsilon) \approx \frac{1}{1 - 1.5} = -2.0$$

C_2 **segment**: referring to Eq. (19),

$z = e^{j\Omega}$ where $0 < \Omega \le (2\pi)^+$. At point $z = e^{j(0^+)}$,

$$G(e^{j(0^+)}) \approx \frac{1}{1 - 1.5} = -2.0$$

At point $z = e^{j\left(\frac{\pi}{2}\right)} = j$,

$$G(j) = \frac{1}{j - 1.5} = \frac{-1.5 - j}{\sqrt{1.5^2 + 1}}$$

At point $z = e^{j(\pi)} = -1$,

$$G(-1) = \frac{1}{-1 - 1.5} = -0.4$$

At point $z = e^{j(2\pi^+)}$,

$$G(e^{j(2\pi^+)}) \approx \frac{1}{1 - 1.5} = -2.0$$

C_{3a} segment is analyzed as C_{1a} segment , whereas the mapping by the C_3 segment is reversed to the one by the C_1 segment. $G(d)$ of the C_3 segment is the same as $G(e)$ of the C_1 segment.

C_4 **segment:** referring to Eq. (35),

$z = re^{-j\Omega}$ where $r \to \infty$ and $0^- \le \Omega \le (2\pi)^-$. From Eq. (36),

$$G(d) = G(re^{-j(0^-)}) \to 0e^{j(0^-)}$$

From Eq. (39),

$$G(e) = G(re^{-j(2\pi^-)}) \to 0e^{j(2\pi^-)}$$

$$\angle G(e) - \angle G(d) = (2\pi)$$

This means that there is an encirclement by $2\pi\ rad$ of a miniature circle around the origin of the $G(z)$ plane starting from point $G(d)$ and continuing to point $G(e)$. The Nyquist sketch of this example can be illustrated as in Figure 5.

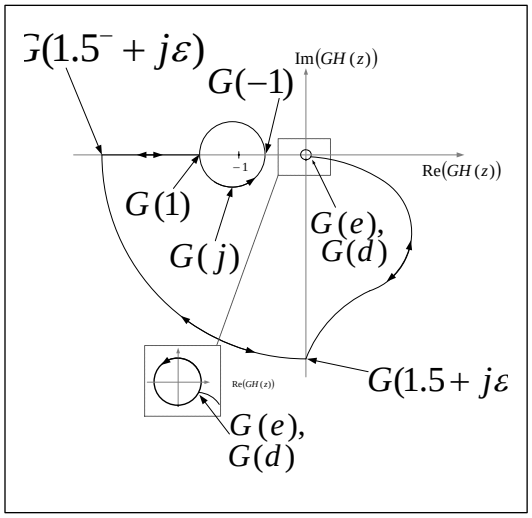

Figure 5. Nyquist plot of $G(z)=\frac{1.0}{z-1.5}$.

From Figure 5, $N=1$ and from $G(z)$, $P=1$, therefore,

$$Z=P-N=1-1=0$$

As a result, this system is stable due to the nonexistence of closed-loop poles (zeros of $1+G(z)$) outside the unit circle in the z-plane complying with the calculation for the zero of $P(z)$ at $z=0.5$.

3.2 Example 2.

Considering a sample-data control system in Fig. 1 with unity feedback $H(s)=1$, let

$$G(z)=\frac{(z-2)(z-2.5)}{(z-1.5)(z-4.5)(z-3\pm 2j)}$$

Poles of $G(z)$ are at: $z=1.5,\ 4.5,\ 3\mp 2j$

Zeros of $G(z)$ are at: $z=2,\ 2.5$

The polynomial form of $G(z)$ is

$$G(z)=\frac{z^2-4.5z+5}{z^4-12z^3+55.75z^2-118.5z+87.75}$$

The characteristic equation, $P(z)$ can be expressed as

$$P(z)=1+G(z)=\frac{z^4-12z^3+56.75z^2-123z+92.75}{z^4-12z^3+55.75z^2-118.5z+87.75}$$

Zeros of $P(z)$ are at :

$z=1.5252,\ \ 4.2430,\ \ 3.1159\pm 2.1502j$

The Nyquist contour can be demonstrated as in Figure 2. The contour consists of 6 segments, namely

C_1 **segment:** referring to Eq. (6),

$z=\frac{1}{r+1}+j\varepsilon$ where $-1\le r\le 0$ and $\varepsilon\to 0(\varepsilon=0^+)$. According to Eq. (8)

$$G(e)\approx 0^+-j\beta$$

Traversing on this segment to the point directly over the pole at $z=4.5$. This point is expressed as $z=4.5+j\varepsilon$

$$G(4.5+j\varepsilon)\to\infty\angle\left(-\frac{\pi}{2}\right)$$

Continuing to point $z=4.5^-+j\varepsilon$

$$G(4.5^-+j\varepsilon)\to\infty\angle(-\pi)$$

Continuing to point $z=2.5+j\varepsilon$

$$G(2.5+j\varepsilon)\to 0\angle\left(-\pi+\frac{\pi}{2}\right)=0\angle\left(-\frac{\pi}{2}\right)$$

Continuing to point $z=2.5^-+j\varepsilon$

$$G(2.5^-+j\varepsilon)\to 0\angle\left(-\frac{\pi}{2}+\frac{\pi}{2}\right)=0\angle(0)$$

Continuing to point $z=2+j\varepsilon$

$$G(2+j\varepsilon)\to 0\angle\left(0+\frac{\pi}{2}\right)=0\angle\left(\frac{\pi}{2}\right)$$

Continuing to point $z=2^-+j\varepsilon$

$$G(2^-+j\varepsilon)\to 0\angle(\pi)=0\angle(\pi)$$

Continuing to point $z=1.5+j\varepsilon$

$$G(1.5+j\varepsilon)\to\infty\angle\left(\pi-\frac{\pi}{2}\right)=\infty\angle\left(\frac{\pi}{2}\right)$$

Continuing to point $z=1.5^{-}+j\varepsilon$

$$G(1.5^{-}+j\varepsilon)\to\infty\angle\left(\frac{\pi}{2}-\frac{\pi}{2}\right)=\infty\angle(0)$$

Continuing to point $z=1.0+j\varepsilon$

$$G(1.0+j\varepsilon)$$
$$\approx\frac{1^2\text{ - }4.5\ +5}{1^4\text{ -}12\ (1^3)+55.75\ (1^2)\text{ -}118.5\ +87.75}$$
$$\approx 0.1071$$

C_{1a} **segment:** referring to Eq. (18), $z=1-r+j\varepsilon$ where $0\le r\le 0^{+}$ and $\varepsilon\to 0(\varepsilon=0^{+})$. At point $z=1.0+j\varepsilon$

$$G(1.0+j\varepsilon)$$
$$\approx\frac{1^2\text{ - }4.5\ +5}{1^4\text{ -}12\ (1^3)+55.75\ (1^2)\text{ -}118.5\ +87.75}$$
$$\approx 0.1071$$

At point $z=1.0^{-}+j\varepsilon$

$$G(1.0^{-}+j\varepsilon)$$
$$\approx\frac{1^2\text{ - }4.5\ +5}{1^4\text{ -}12\ (1^3)+55.75\ (1^2)\text{ -}118.5\ +87.75}$$
$$\approx 0.1071$$

C_2 **segment**: referring to Eq. (19), $z=e^{j\Omega}$ where $0<\Omega\le(2\pi)^{+}$. At point $z=e^{j(0^{+})}$,

$$G(e^{j(0^{+})})$$
$$\approx\frac{1^2\text{ - }4.5\ +5}{1^4\text{ -}12\ (1^3)+55.75\ (1^2)\text{ -}118.5\ +87.75}$$
$$\approx 0.1071$$

At point $z=e^{j\left(\frac{\pi}{2}\right)}=j$,

$$G(j)$$
$$=\frac{\mathrm{j}^2\text{ - }4.5\ \mathrm{j}+5}{\mathrm{j}^4\text{ -}12\ \mathrm{j}^3+55.75\ \mathrm{j}^2\text{ -}118.5\ \mathrm{j}+87.75}$$
$$=\frac{4-4.5j}{1-55.75+87.75-12j-118.5j}$$
$$=\frac{4-4.5j}{33-130.5j}=0.0492+0.0223j$$

At point $z=e^{j(\pi)}=-1$,

$$G(-1)$$
$$=\frac{(-1)^2\text{ - }4.5\ (-1)+5}{(-1)^4\text{ -}12\ (-1)^3+55.75\ (-1)^2\text{ -}118.5\ (-1)+87.75}$$
$$=0.0382$$

At point $z=e^{j(2\pi^{+})}$,

$$G(e^{j(2\pi^{+})})$$
$$\approx\frac{1^2\text{ - }4.5\ +5}{1^4\text{ -}12\ (1^3)+55.75\ (1^2)\text{ -}118.5\ +87.75}$$
$$\approx 0.1071$$

C_{3a} segment is analyzed as C_{1a} segment , whereas the mapping by the C_3 segment is reversed to the one by the C_1 segment. $G(d)$ of the C_3 segment is the same as $G(e)$ of the C_1 segment.

C_4 **segment:** referring to Eq. (35), $z=re^{-j\Omega}$ where $r\to\infty$ and $0^{-}\le\Omega\le(2\pi)^{-}$. From Eq. (36),

$$G(d)=G(re^{-j(0^{-})})\to 0e^{j(0^{-})}$$

From Eq. (39),

$$G(e)=G(re^{-j(2\pi^{-})})$$
$$\to 0e^{j((8\pi^{-})-(4\pi^{-}))}=0e^{j(4\pi^{-})}$$

$$\angle G(e)-\angle G(d)=(4\pi)$$

This means that there is an encirclement by $4\pi\ rad$ of a miniature circle around the origin of the $G(z)$ plane starting from point $G(d)$ and continuing to

point $G(e)$. The Nyquist sketch of this example can be illustrated as in Figure 6. From Figure 6, $N = 0$ and from $G(z)$, $P = 4$, therefore,

$$Z = P - N = 4 - 0 = 4$$

As a result, this system is unstable due to the existence of closed-loop poles (zeros of $1 + G(z)$) outside the unit circle in the z-plane complying with the calculation for the zeros of $P(z)$ at $z = 1.5252,\ 4.2430$, $3.1159 \pm 2.1502\text{j}$.

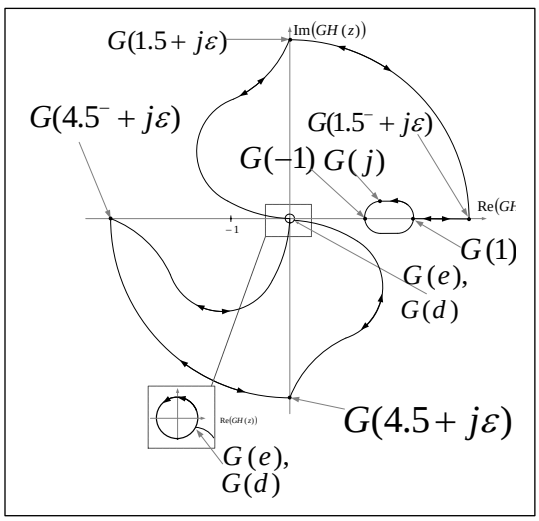

Figure 5. Nyquist plot of $G(z) = \dfrac{(z-2)(z-2.5)}{(z-1.5)(z-4.5)(z-3\pm 2j)}$

4. Conclusion

On the ground of the Nyquist contours proposed by many literatures, real poles and zeros of the loop pulse transfer function, $GH(z)$, outside the unit circle in the z-plane are always excluded, leading to the wrong result of the relative stability test by the Nyquist stability criterion; however, this study proposes a new Nyquist contour that can incorporate those real poles and zeros. In addition, the encirclement around the point $GH(z) = -1$ of the mapping by $GH(z)$ is influenced mainly by the C_2 segment which is the unit circle in the z-plane. The relative stability analysis results by this contour are confirmed by two examples in Section 3 that can handle the case of complex conjugate poles and zeros outside the unit circle in the z-plane as well. Nevertheless, the study scope focuses on the case of real poles and zeros of the loop pulse transfer function, $GH(z)$, outside the unit circle. Future work will include coverage of the complex conjugate poles and zeros on the unit circle and real poles and/or zeros at $z = 1$ in the z-plane.

5. References

[1] H. Nyquist, Regeneration Theory, Bell System Technical Journal, vol. 11, 1932.

[2] F. Golnaraghi and B. C. Kuo, Automatic Control Systems, River Street, Hoboken, NJ: John Wiley & Sons, Inc.,, 2010.

[3] M. Gopal, Control Systems: Principles and Design, Singapore: Tata McGraw-Hill, 2002.

[4] C. L. Phillips and H. T. Nagle, Digital Control System Analysis and Design, Upper Saddle River, NJ: Pearson Education International Inc., 1998.

[5] Module 5: Design of Sampled Data Control Systems Lecture Note 4, Available Source: http://nptel.ac.in/courses/108103008/PDF/module5/m5_lec4.pdf.

[6] T. Berlin, Analysis of Discrete-Time Systems, Available Source: http://www.control.tu-berlin.de/images/0/0b/DCS_ADTS.pdf, 2014.

[7] M. S. Fadali and A. Visioli, Digital Control Engineering: Analysis and Design, Waltham, MA: Academic Press, Elsevier, 2013.

[8] K. Glover and R. Sepulchre, Discrete Time Systems (Lectures 1--6), Available Source: http://www-control.eng.cam.ac.uk/foswiki/pub/Main/RodolpheSepulchre/3F1_2RS.pdf, 2013.
[9] B. D. Moor, Chapter 11: Design in the frequency domain, Nyquist stability criterion, Available Source: http://homes.esat.kuleuven.be/~maapc/Sofia/slides_chapter11.pdf, 2015.
[10] M. S. Fadali, Stability of Digital Control Systems, Available Source: https://www.coursehero.com/file/10095701/ch-4-Stability/.